Environ. Sci. Technol. **1999**, *33,* 560−570

Kinetic Model To Describe the Intrinsic Uncoupling Activity of Substituted Phenols in Energy Transducing Membranes

BEATE I. ESCHER,*
RENÉ HUNZIKER, AND
RENÉ P. SCHWARZENBACH
Swiss Federal Institute for Environmental Science and Technology (EAWAG), and Swiss Federal Institute of Technology (ETH), CH-8600 Dübendorf, Switzerland

JOHN C. WESTALL
Oregon State University, Corvallis, Oregon

A new approach to understand the increased toxicity of uncouplers as compared to baseline toxicity (narcosis) is presented here. The overall uncoupling activity is quantitatively separated into the contribution of membrane concentration and speciation and intrinsic activity. This approach is a further step toward the development of improved Quantitative Structure−Activity Relationships (QSAR) and of toxicokinetic models used in risk assessment. The protonophoric uncoupling activity of seven nitro- and chlorophenols has been investigated as a function of pH and concentration using time-resolved spectroscopy on photosynthetic membranes. The experimental data are described by a kinetic model that includes a monomeric and a dimeric protonophoric shuttle mechanisms. Input parameters of the model are the experimental data for relaxation of the membrane potential, the biomembrane-water distribution constants of the phenol and phenoxide species, and the acidity constant of the phenol. Adjustable parameters are the translocation rate constants of all phenolic species and the heterodimer formation constant. These parameters constitute the intrinsic uncoupling activity. Hydrophobicity and acidity govern the partitioning of phenols into the membrane but appear not to be the sole determining factors for the intrinsic uncoupling activity of phenolic compounds. Additional factors include steric effects and charge distribution within the molecule.

Introduction

For the development of predictive toxicity models it is important to identify and understand the mechanism of toxicity (*1*). The toxicity of nonspecifically acting compounds (narcotics) is a direct function of the amount of chemical present in the organism (*2*) and can be predicted from their hydrophobicity by Quantitative Structure−Activity Relationships (QSAR). Other compounds exhibit toxicity greater than that predicted from QSARs of narcotic baseline toxicity (*3*). For these compounds, predictive models have to account for the ability of a compound already present at the target site to act according to a specific mechanism. The toxic activity of such a specifically acting compound, normalized to its concentration at the target site, is referred to as the "intrinsic toxicity" of the compound.

A large number of phenolic compounds and other hydrophobic ionogenic organic compounds (HIOCs) act specifically by interfering with one of the basic cellular functions, namely, energy transduction. In energy-transducing membranes, HIOCs may inhibit the electron flow by binding directly to specific components of the electron-transfer chain (*4*), and, even more importantly, they can destroy the electrochemical proton gradient by transporting protons across the membrane thereby short-circuiting the chemiosmotic proton cycle and preventing ATP synthesis (*5, 6*). This mechanism is commonly referred to as uncoupling of oxidative- or photophosphorylation or simply "uncoupling".

In the case of phenolic compounds and other weak organic acids, the mechanism of uncoupling is viewed as a shuttle mechanism, in which both the neutral phenol species and the charged phenoxide act together to transport protons across the membrane. In addition, a heterodimer composed of one phenol plus one phenoxide species can participate as charge carrier in the shuttle mechanism (*7*). The model of the protonophoric shuttle mechanism is sketched in Figure 1. The charged species migrate across the membrane driven by the membrane potential. Protons are then taken up from the aqueous phase, and the resulting neutral phenols diffuse back across the membrane driven by the concentration gradient of phenols that has been built up by the migration processes. Hence, the overall uncoupling activity of a given phenol is dependent not only on its total concentration in the membrane (as is the case for narcotic effects) but also on its speciation in the membrane (i.e., degree of dissociation and formation of heterodimers) and the abilities of the various species to cross the membrane. These transport characteristics, or the ability of the compound already present in the membrane to relax the electrochemical proton gradient across the membrane, corresponds to the intrinsic uncoupling activity.

In earlier work, we have shown that time-resolved spectroscopy can be used to quantify the uncoupling activity of phenols in photosynthetic membranes of the purple bacterium *Rhodobacter sphaeroides* (*4*). In this test system, the membrane potential is created by a brief, "single-turnover" flash of light. The build-up and the subsequent relaxation of the membrane potential is deduced from the change in absorbance at 503 nm (*8*). Uncouplers increase the relaxation rate. The uncoupling activity can be expressed as the pseudo-first-order rate constant for the decay of absorbance (and hence membrane potential).

In a subsequent study we related the first-order decay constants of a large number of chloro- and nitrophenols to the concentration of the phenol and phenoxide species sorbed into the membrane at pH 7 (*9*) by combining the results of the earlier study with results of membrane-water partitioning experiments (*10*). This first crude analysis of the data already provided some interesting insight into the factors that determine the overall uncoupling activity of a given compound and pointed to the fact that there are activity differences between the different phenols in addition to the effect of membrane concentration and speciation. However, the simple model failed to describe adequately the effect of pH on the uncoupling activity of the compounds.

In the work presented in this paper, we measured the pH-dependence of the uncoupling activity of seven chloro- and nitrophenols with the goal of assessing the relative

* Corresponding author phone: 0041-1-823 5068; Fax: 0041-1-823 5471; e-mail address: escher@eawag.ch.

10.1021/es980545h CCC: $18.00
Published on Web 01/06/1999

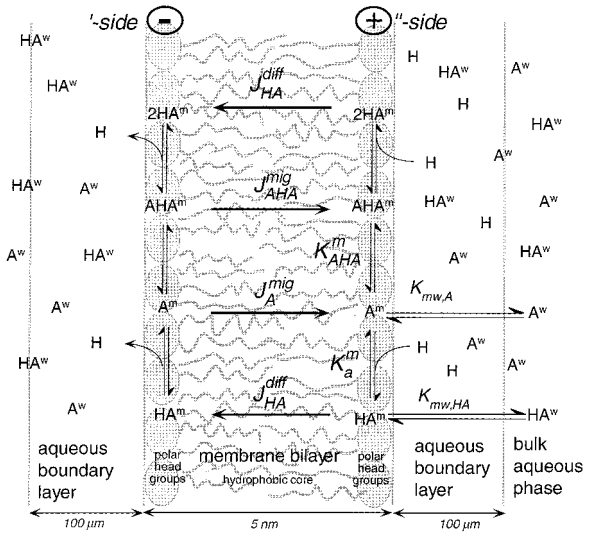

FIGURE 1. Model for protonophoric shuttle mechanism of weak organic acids. Slow equilibrium processes before the experiment are the distribution of the neutral acid HA^w and the charged conjugated base A^w into the polar headgroups of the lipid bilayer described by $K_{mw,HA}$ and $K_{mw,A}$. During the experiment, the concentrations of HA^m, A^m, and the heterodimer AHA^m in the membrane are rapidly equilibrated according to the acidity constant K_a^m and the heterodimer formation constant K_{AHA}^m. The translocation processes across the membrane involved are the diffusion of HA^m, J_{HA}^{diff}, and the migration of A^m, J_A^{mig}, and of AHA^m, J_{AHA}^{mig}.

contributions of various factors (i.e., membrane-water partitioning, speciation inside the membrane, transport rates of the various species) to the pH-dependent effect of a given compound. The model described in this paper is an extension of biophysical models used in the past to describe the kinetics of the protonophoric shuttle mechanism of weak organic acids in artificial planar lipid bilayers (*11*, *12*). It is shown that the experimental data can be adequately described with this model, and that translocation rate constants can be deduced for all species involved. The results of this study demonstrate that for developing improved QSARs for specifically acting chemicals and for assessing possible synergistic effects of such compounds in mixtures, it is necessary to separate target site (membrane) concentration from intrinsic activity.

Uncoupling Model

Description of the Protonophoric Uncoupling Process. The observed rate constant of the exponential decay in absorbance at 503 nm, k_{obs}, is the experimental measure of the uncoupling activity. To explain the dependence of k_{obs} on pH and total concentration of phenol in the aqueous phase, we present a new kinetic model of a protonophoric shuttle mechanism of uncoupling. This model was adapted from the kinetic transport model of acidic uncouplers in artificial planar lipid bilayer membranes used by McLaughlin and co-workers (*11*−*14*). Our model relies on a number of assumptions introduced by McLaughlin et al. (*11*−*14*), extends that work closer to a real biological system, and accounts for possible heterodimer formation. In this section, the assumptions and the essential features of the model are described for weak organic acids. A general derivation is presented in the Appendix.

Figure 1 gives an overview of the relevant processes considered in the kinetic uncoupling model. The neutral acid HA and the charged conjugate base A are in equilibrium between the aqueous phase and the surface layers on both sides of the chromatophore membrane. At equilibrium, the concentrations in the aqueous phases adjacent to the ′-side and the ″-side of the membrane are equal, as they are in the membrane phase at ′ and ″. During a typical experiment (<1 s) the membrane can be considered to be temporarily isolated from the aqueous solution, because the permeability of the membrane (thickness approximately 5 nm) to all organic molecules is at least 3 orders of magnitude greater than the permeability of the unstirred aqueous boundary layer adjacent to the membrane (thickness 100 μm) (*6*). The proton is assumed to be the only species that moves between the bulk aqueous phases supposedly by a "buffer shuttle" mechanism through the unstirred aqueous layer (*11*).

In the excitation phase of the experiment, the flash of light causes rapid transport of electrons from the ″-side to the ′-side of the membrane through a series of oxidation−reduction reactions followed by a slower transfer of protons from the ′-side to the ″-side thereby building up a surface charge and the membrane potential, $\Delta\phi$. Because the concentrations of all uncoupler species, both in the membrane and in solution, are small compared to the concentrations of buffer ions in solution, and the buffer capacity in the aqueous phase is high, the charge created by the transport of protons across the membrane is presumed to be accommodated by slight shifts in the buffer speciation, while the pH remains constant.

During the relaxation phase, only the processes occurring within the membrane have to be considered. The charged species, phenoxide A^m and heterodimer AHA^m (where the superscript m represents the membrane), migrate along the membrane potential from the ′-side to the ″-side of the membrane. At the membrane-water interfaces, the acid−base equilibrium is maintained, and protons are exchanged with the buffer or water in the aqueous boundary layer (*14*). The acid−base and heterodimer formation reactions are fast compared to the diffusion of the molecules across the membrane (*11*). Therefore, it can be assumed that these reactions are in equilibrium at any time during the experiment. Then, the neutral species HA^m diffuses back across the membrane from the ″-side to the ′-side along the concentration gradient that is built up as a result of the migration processes. Ultimately the initial equilibrium state is regained.

Speciation in the Aqueous Phase (w). The organic acid dissociates in the aqueous phase according to the reaction

$$HA^w \rightleftharpoons H + A^w \tag{1}$$

where HA^w represents the neutral protonated form, A^w the acid anion, and H the aqueous hydrogen ion, and K_a^w is the equilibrium constant. Representations of positive charge of proton and negative charge of phenoxide are omitted for brevity. The mass law expression for this reaction is

$$K_a^w = \frac{C_A^w a_H}{C_{HA}^w} \tag{2}$$

where C_A^w and C_{HA}^w (mol·L^{-1}) represent the concentrations of A and HA in the aqueous phase and a_H the hydrogen activity (pH = −log a_H), and the total concentration in the aqueous phase C_{tot}^w is defined by

$$C_{tot}^w = C_{HA}^w + C_A^w \tag{3}$$

Concentration and Speciation in the Membrane (m). Both the species HA and A partition between the aqueous phase and membrane phase according to reactions of the type

$$HA^w \rightleftharpoons HA^m \quad (4)$$

$$A^w \rightleftharpoons A^m \quad (5)$$

where HA^m and A^m refer to the species in the membrane. The mass law equations for these reactions are

$$K_{mw,HA} = \frac{C^m_{HA}}{C^w_{HA}} \quad (6)$$

$$K_{mw,A} = \frac{C^m_A}{C^w_A} \quad (7)$$

where C^m_A and C^m_{HA} are the effective concentrations in the membrane phase in units of mol of HA or A per kg of phospholipid in the membrane.

Furthermore, HA and A are postulated to react in the membrane to form the negatively charged heterodimer, AHA,

$$HA^m + A^m \rightleftharpoons AHA^m \quad (8)$$

for which the mass law expression is

$$K^m_{AHA} = \frac{C^m_{AHA}}{C^m_{HA} \cdot C^m_A} \quad (9)$$

The total concentration of uncoupler in the membrane, C^m_{tot}, is the sum of the concentrations of all these species

$$C^m_{tot} = C^m_{HA} + C^m_A + 2C^m_{AHA} \quad (10)$$

and the total concentration of uncoupler in the system, C_{tot}, is

$$C_{tot} = C^m_{tot} \cdot [m] + C^w_{tot} \quad (11)$$

where [m] is the ratio of membrane lipid to aqueous phase expressed in units of kg phospholipid per liter.

It is convenient to define the fractions of the different phenolic species present in the aqueous phase and inside the membrane, α^w_i and α^m_i , respectively, at a given pH

$$\alpha^w_i = \frac{C^w_i}{C^w_{tot}} \quad (12)$$

$$\alpha^m_i = \frac{C^m_i}{C^m_{tot}} \quad (13)$$

Substitution of eqs 3 and 10 in eq 11 yields a complete mass balance. All species concentrations are then reexpressed in terms of C^w_{HA} and the relevant mass law equations.

$$C_{tot} = C^w_{HA} + C^w_{HA}\frac{K_a}{a_H} + C^w_{HA}K_{mw,HA}[m] + C^w_{HA}K_{mw,A}\frac{K_a}{a_H}[m] + 2C^w_{HA}K_{mw,HA}C^w_{HA}\frac{K_a}{a_H}K^m_{AHA}[m] \quad (14)$$

The resulting quadratic equation is solved for C^w_{HA}, from which the concentrations of all species and the values of α^w_i and α^m_i can be calculated. The values of α^m_A, α^m_{HA}, and α^m_{AHA} so calculated are exact for the initial equilibrium condition, and are a very good approximation of the speciation during excitation and relaxation if the C^m_{AHA} term is negligible in eq 10 or the relative changes in total concentration of phenol at both sides of the membrane are small following a flash. As will be shown, these conditions are generally met. There is evidence that the C^m_{AHA} term is negligible compared to the sum of C^m_{HA} and C^m_A. Barstad et al. (*15*) detected AHA heterodimers in non-hydrogen-bonding solvents but were unable to detect AHA in lipid bilayers in aqueous solution. They estimated K^m_{AHA} for pentachlorophenol to lie between 0.005 kg·mol^{-1} and 0.5 kg·mol^{-1} from a combination of membrane conductivity measurements and the surface density of adsorbed PCP. Since the heterodimer can migrate more easily across the membrane than the anionic monomer, it may contribute significantly to the overall process despite its low concentration (*7*).

Finally, the acid−base reaction in the membrane is defined by the reaction

$$HA^m \rightleftharpoons H + A^m \quad (15)$$

for which the mass law expression is

$$K^m_a = \frac{C^m_A a_H}{C^m_{HA}} = K^w_a \frac{K_{mw,A}}{K_{mw,HA}} \quad (16)$$

Note that the acidity constant in the membrane phase K^m_a is operationally defined in terms of the proton activity in the aqueous phase, because we assume that there are no free protons in the membrane and that the protons of the acid−base reaction in the membrane are directly exchanged with the adjacent aqueous solution.

The equations above refer to the bulk partitioning and speciation of the acid in the solution and in the membrane. However, both neutral and charged species are assumed to be located primarily near the surface of the membrane, at the interface between polar headgroups and hydrophobic membrane core (*16*, *17*). Therefore, the bulk membrane concentrations of a species i can be converted to surface-normalized concentrations on each side of the membrane, Γ_i (mol·m^{-2}), by dividing C^m_i by the specific surface area, *s*, of the phospholipids in the chromatophore membrane

$$\Gamma_i = \frac{C^m_i}{s} \quad (17)$$

$$s = \frac{N_A A}{m_{PL}} \quad (18)$$

where the average molecular weight of the phospholipids in chromatophores m_{PL} is 760 g·mol^{-1} (*18*), N_A is the Avogadro number, and the average surface area *A* of one phospholipid in a membrane is approximately 5 to 6 × 10^{-19} m^2 (*19*). The resulting specific surface area *s* is 4.4 × 10^5 m^2 kg^{-1}.

General Membrane Transport. The flux of species i, J_i [mol·m^{-2}·s^{-1}], from ′ across the membrane to ″ is defined by the first-order translocation expression

$$J_i = \frac{-d\Gamma'_i}{dt} = \frac{d\Gamma''_i}{dt} \quad (19)$$

The driving force of the flux of species i is on one hand the concentration gradient that causes the diffusional flux J^{diff}_i (translocation independent of electric field) and on the other hand the membrane potential that causes the migrational flux J^{mig}_i (translocation of charged species in an electric field)

$$J^{diff}_i = -k_i\Gamma''_i + k_i\Gamma'_i \quad (20)$$

$$J^{mig}_i = -k_i z_i\left(\frac{\Gamma'_i + \Gamma''_i}{2}\right)\Delta u \quad (21)$$

where k_i is a homogeneous translocation coefficient expressed

in units of s^{-1}, z_i is the charge of species i, $(\Gamma_i' + \Gamma_i'')/2 = \Gamma_i^0$ corresponds to the total surface concentration of species i, and Δu is the dimensionless membrane potential defined by

$$\Delta u = \frac{F\Delta\phi}{RT} \tag{22}$$

where $\Delta\phi$ is the membrane potential $(\phi'' - \phi')[V]$, F is the Faraday constant, R is the gas constant, and T is the temperature. The sum of the diffusional and the migrational flux constitutes the total flux J_i

$$J_i = J_i^{diff} + J_i^{mig} = -k_i\Gamma_i''\left(1 + \frac{\Delta u}{2}z_i\right) + k_i\Gamma_i'\left(1 - \frac{\Delta u}{2}z_i\right) = -2k_i\Delta\Gamma_i - k_i z_i\Gamma_i^0\Delta u \tag{23}$$

where $\Delta\Gamma_i = (\Gamma_i'' - \Gamma_i')/2$.

It remains to relate the membrane potential to surface concentrations. The membrane potential is related to the surface charge, σ, as in a parallel plate capacitor

$$\Delta\phi = C^{-1}\sigma \tag{24}$$

where C is the capacitance of the chromatophore membrane of approximately $5.5\cdot10^{-3}$ F m^{-2} (*19*). The change in surface charge σ is a function of the flux of the charged species.

$$\frac{d\sigma}{dt} = F\sum_i z_i J_i \tag{25}$$

Equations 1−25 define the uncoupling model. As shown in the Appendix, rearrangement of eqs 1−25 yields two coupled differential equations (eqs 41 and 43), for which the eigenvalues λ_1 and λ_2 (eq 47) are the characteristic times to be compared to k_{obs}. The rate constants of decay are a function of the experimental conditions (total organic acid concentration, total concentration of phospholipid, pH), three independently determined parameters describing membrane concentration and speciation ($K_{mw,HA}$, $K_{mw,A}$, and pK_a^w), and the adjustable parameters describing the intrinsic activity (k_{HA}, k_A, k_{AHA}, and K_{AHA}^m).

The model described above predicts a biphasic decay in membrane potential with characteristic times corresponding to the values of λ_1 and λ_2. This biphasic decay could be observed in charge-pulse experiments on artificial lipid membranes (*11*). For the movement of tetraphenylborate ions across black lipid membranes under charge-pulse conditions, the fast phase λ_2 was attributed to the displacement of lipophilic ions as a consequence of the suddenly applied voltage, whereas the second slow voltage relaxation λ_1 represents the slow discharge of the membrane through the external resistor and the redistribution of charges within the membrane (*13*).

However, the faster phase of the decay, which is described by the greater eigenvalue λ_2, was too fast to be detected with the experimental system described here. Since the build-up of the membrane potential is polyphasic with half-times of the spatial electron-transfer reactions from picoseconds to milliseconds (*20*), decay rate constants ≥ 70 s^{-1} cannot be resolved. Consequently, the values of the adjustable parameters were derived from a nonlinear fit of the observed monophasic decay rate constants (k_{obs}) to the calculated values of λ_1 (eq 47), for sets of experiments in which both the pH value and the total concentration of organic acid were varied.

Transport Processes for Acidic Uncouplers. From the general equations given above, the equations for acidic uncouplers that can additionally form heterodimers can be set up. The diffusional flux of the neutral species, J_{HA}^{diff} is

$$J_{HA}^{diff} = -2k_{HA}\Delta\Gamma_{HA} \tag{26}$$

The diffusional fluxes of the phenoxide, J_A^{diff}, and of the heterodimer, J_{AHA}^{diff}, are defined analogously and are implemented as well in the uncoupling model. The modeling results show, however, that these latter fluxes are rather small under most experimental conditions. The migrational fluxes of the charged species, J_A^{mig} and J_{AHA}^{mig}, are defined according to

$$J_A^{mig} = -k_A\Gamma_A^0\Delta u \tag{27}$$

$$J_{AHA}^{mig} = -k_{AHA}\Gamma_{AHA}^0\Delta u \tag{28}$$

If the back-diffusion of the neutral species did not influence the overall uncoupling mechanism, the uncoupling model could be simplified to the migration of the charged species, and k_{obs} would be a linear combination of the contribution from phenoxide and heterodimer:

$$k_{obs} = k_A\Gamma_A^0 + k_{AHA}\Gamma_{AHA}^0 \tag{29}$$

In this case, the experimental data, k_{obs}, can be related to the total concentration of phenol added to the system, C_{tot}, from the quadratic equation

$$k_{obs} = a\cdot C_{tot} + b\cdot C_{tot}^2 \tag{30}$$

This simple equation was used in a previous study (*9*) to describe the concentration dependence of k_{obs} at constant pH and is still applied in the present study to identify the relevant charged species of a given compound. Note, however, that for all data presented here, the back-diffusion of HA had a significant contribution to the overall uncoupling process and could not be set to indefinite.

Material and Methods

Chemicals. The phenols (full names and abbreviations are given in Table 1) were purchased from the following companies: Riedel-de Häen (Seelze, Germany): 245TCP, DINOSEB, DINOTERB; Fluka (Buchs, Switzerland): 345TCP, 2345TeCP, PCP, 34DNP. The following biological buffers were used: MES (2-morpholino-ethanesulfonic acid, $pK_a = 6.15$); MOPS (3-(*N*-morpholino)propanesulfonic acid, $pK_a = 7.2$); HEPPS (*N*-2-hydroxyethylpiperazine-*N*′-3-propanesulfonic acid, $pK_a = 7.8$); CHES (2-(cyclohexylamino)ethanesulfonic acid, $pK_a = 9.55$), all of which were from Fluka (Buchs, Switzerland). Chemicals used for time-resolved spectroscopy are described in ref *4*.

Determination of the Uncoupling Activity. Membrane vesicles (chromatophores) of the purple bacterium *Rhodobacter sphaeroides* were prepared and characterized as described previously (*4*, *21*). The single-beam spectrophotometer equipped with a flash excitation unit and kinetic data acquisition capabilities is described elsewhere (*4*). The measurements were performed in an anaerobic cuvette at a redox potential adjusted to 120−130 mV with redox mediators (2,3,5,6-tetramethyl-phenylene diamine, *N*-methyl phenazonium methosulfate, duroquinone, 1,2-naphthoquinone, 1,4-naphthoquinone) and ferricyanide/dithionite in a buffer composed of a mixture of MES, MOPS, HEPPS, and CHES, adjusted to a total buffer- and K^+ concentration (KCl/KOH) of 50 mM and 100 mM, respectively. Since the buffer mixture did not buffer equally well at every point and the stock suspension of chromatophores was prepared in a buffer of pH 7, the pH was measured at the end of each series directly in the cuvette. Deviation from the initial value was never larger than ± 0.2 pH-units. At each pH-value, several measurement cycles with different total concentrations of phenol were performed. During one measurement cycle, four

TABLE 1. Summary of All Parameters That Determine the Uncoupling Model

compound	abbreviation	$K_{mw,HA}$[a] ($L \cdot kg^{-1}$)	pK_a^w	K_{mw,A^-} ($L \cdot kg^{-1}$)	k_{HA} (s^{-1})	k_A (s^{-1})	k_{AHA}[i] (s^{-1})	range of C_{tot} (μM)[k]	n[l]
3,4-dinitrophenol	34DNP	$1.47 \cdot 10^3$	5.38[b]	$(7.51 \pm 2.28^f) \cdot 10^2$ [g]	82 ± 23	0.07 ± 0.01	53 ± 10	5−100	102
2-*sec*-butyl-4,6-dinitrophenol	DINOSEB	$9.45 \cdot 10^3$	4.62[c]	$2.16 \cdot 10^3$ [a]	1005 ± 151	0.48 ± 0.03	0[j]	2−10	36
2-*tert*-butyl-4,6-dinitrophenol	DINOTERB	$1.26 \cdot 10^4$	4.80[d]	$3.89 \cdot 10^3$ [a]	6006 ± 697	1.45 ± 0.11	0[j]	0.1−40	78
2,4,5-trichlorophenol	245TCP	$2.18 \cdot 10^4$	6.94[e]	$(1.05 \pm 0.13) \cdot 10^4$ [g]	142 ± 816	0.014 ± 0.001	10.0 ± 0.9	2−70	50
3,4,5-trichlorophenol	345TCP	$5.13 \cdot 10^4$	7.73[e]	$(2.46 \pm 0.36) \cdot 10^4$ [g]	150[h]	0.09 ± 0.01	21.6 ± 2.6	2−30	43
2,3,4,5-tetrachlorophenol	2345TeCP	$7.80 \cdot 10^4$	6.35[e]	$(3.44 \pm 0.59) \cdot 10^4$ [g]	108 ± 29	0.19 ± 0.02	157 ± 20	1−8	52
pentachlorophenol	PCP	$1.23 \cdot 10^5$	4.75[e]	$3.09 \cdot 10^4$ [a]	346 ± 24	0.17 ± 0.09	0[j]	1−50	101

[a] Data from ref *10*. [b] Experimentally determined. [c] $I = 50$ mM (*25*). [d] $I = 250$ mM, 1% methanol mM (*27*). [e] $I = 10$ and 50 mM (*26*). [f] Standard error. [g] Fitted. [h] pK_a^m is at the limit of acceptable range that there is no convergence of fit unless k_{HA} is fixed to an estimated value (approximately equal to the value of 245TCP). [i] Value refers to k_{AHA} if K_{AHA}^m is set to 1 kg L^{-1}, i.e., more precisely, the values in this column correspond to the product of $k_{AHA} \cdot K_{AHA}^m$. [j] Fixed to zero because of linear dependence of k_{obs} from C_{tot}. [k] Concentration range of experimental measurements; membrane lipid concentration in the assay varied between 7.5 and $8.1 \cdot 10^{-4}$ kg·L^{-1}. [l] Number of measurements.

kinetic traces were averaged, each of which consisted of the relative absorption change at 503 nm over a 150 ms intervall, beginning 2 μs after the xenon flash, followed by 1 min of reequilibration. The absorbance change at 503 nm is proportional to the membrane potential (*22*). The membrane potential accounts for the majority of the electrochemical proton gradient in chromatophores (after single-turnover flash $\Delta pH \approx 0.003$, $\Delta\phi \approx 70$ mV) (*23*).

The "uncoupling activity" was quantified as the pseudo-first-order decay rate constant, k_{obs}, of the absorbance at 503 nm and hence of the membrane potential. The value of k_{obs} is normalized via a control for the properties of a particular chromatophore preparation. For more details see refs *4* and *9*. No second faster phase of decay could be resolved despite the model predictions due to interference with the build-up of the membrane potential and large scattering of the kinetic traces.

Determination of Acidity Constants. In the uncoupling model, the acid−base equilibrium in the aqueous phase is defined by the mixed acidity constant at an ionic strength of 100 mM (eq 2). The mixed acidity constant of 34 DNP was determined with a potentiometric titrator (PCA 101, Sirius Analytical Intruments, Riverside, UK) (*24*). The other pK_a^w values were taken from literature (*25*−*27*). In all references, the values refer to mixed acidity constants. Since the exact ionic strength was not given in all cases, and since the estimated error due to differences in ionic strength are estimated to be smaller than 1%, the values given in refs *25*−*27* were directly used.

Determination of Membrane-Water Distribution Ratios. Liposomes prepared from phosphatidylcholine were used as model systems for the determination of the chromatophore-water distribution ratios. Substituted phenols were found to partition nearly quantitatively into the lipid moiety of the chromatophore membrane and uptake into the protein moiety was negligible (*10*). Liposome-water distribution ratios of 34DNP were measured as described in (*10*) as a function of concentration, pH and ionic strength. All other experimental data were taken from ref *10*. The membrane-water distribution coefficients of the neutral phenol, $K_{mw,HA}$, and of the phenoxide, $K_{mw,A}$, were calculated from the experimental values with an improved membrane-water partitioning model (*28*). The improved model is superior to the previously published version (*10*), which was just an extension of the octanol−water partitioning model. In the improved version, the membrane-water distribution is treated as a surface sorption process and not as a bulk partitioning process and therefore does not include ion-pair formation in the lipid bilayer. The resulting distribution ratios for an ionic strength of 100 mM are listed in Table 1.

For some compounds (34DNP, 245TCP, 345TCP, and 2345TeCP), the experimentally determined $K_{mw,A}$ led to an underestimation of the contribution of the charged species in the uncoupling model. Therefore, $K_{mw,A}$ was also used as an adjustable parameter, and the $K_{mw,A}$ determined from the relaxation experiment turned out to be somewhat higher than the experimentally determined $K_{mw,A}$. It is possible that the experimentally determined $K_{mw,A}$, which were measured with pure phosphatidylcholine membranes, underestimate the true uptake of charged species in the chromatophore membrane, 30% of which consists of various different phospholipids (23% phosphatidylcholine, 35% phosphatidylethanolamine, 34% phosphatidylglycerol, 4% cardiolipin, and 3% phosphatidic acid (*18*)) and 70% of which are integral membrane proteins (*9*).

An attempt was made to determine distribution ratios directly with chromatophore membranes (unpublished results), but the pH range of the experiments was too limited to allow the extrapolation of the distribution ratios of the species HA and A.

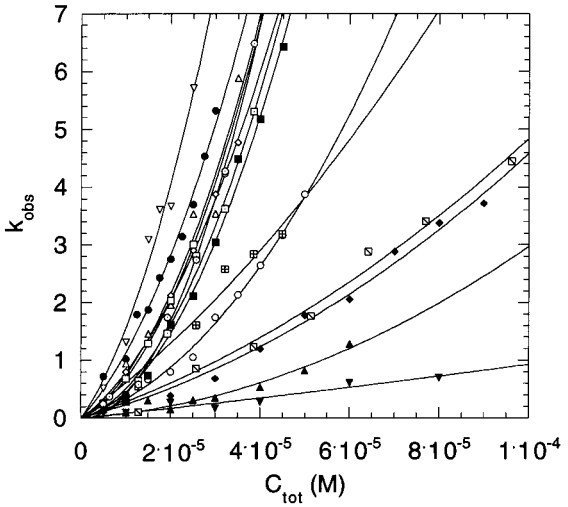

FIGURE 2. Plot of k_{obs} versus the total concentration of uncoupler 34DNP, C_{tot}, at different pH-values, ● pH 5.3, ▽ pH 5.6, △ pH 6.05, ⊙ pH 6.18, ◇ pH 6.33, ⊡ pH 6.42, □ pH 6.5, ○ pH 6.89, ⊞ pH 6.90, ■ pH 6.94, ⧅ pH 7.31, ♦ pH 7.35, ▲ pH 7.82, ▼ pH 8.25. Solid lines are best fits to the simplified quadratic model (eq 30).

Results and Discussion

Determination of the Adjustable Model Parameters. The experimental data consisted of a set of observed rate constants, k_{obs}, determined as a function of total concentration of phenol in the chromatophore suspension, C_{tot}, and of pH, as illustrated for 34DNP in Figure 2 (see Table 1 for abbreviations of compound names). The lines in Figure 2 are the fits of the quadratic model (eq 30). This simplified

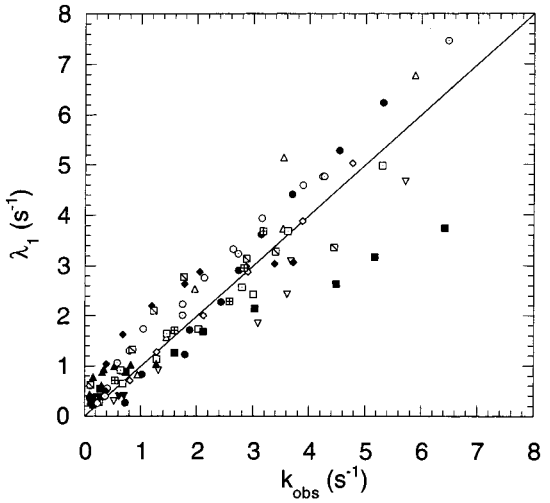

FIGURE 3. Calculated λ_1 versus the experimentally determined k_{obs} for 34DNP; λ_1 were calculated with eq 47 using the parameters listed in Table 1, ● pH 5.3, ▽ pH 5.6, △ pH 6.05, ⊙ pH 6.18, ◇ pH 6.33, ⊡ pH 6.42, □ pH 6.5, ○ pH 6.89, ⊞ pH 6.90, ■ pH 6.94, ⧅ pH 7.31, ♦ pH 7.35, ▲ pH 7.82, ▼ pH 8.25.

model was used to obtain preliminary information on the relevant charged species. A linear dependence of k_{obs} from C_{tot} indicates that the monomer is the dominant charged species, and a purely quadratic dependence of k_{obs} on C_{tot} indicates that the heterodimer is the dominant charged species. If both linear and quadratic term are significant, as is the case for 34DNP, both monomer and heterodimer are assumed to contribute significantly to the protonophoric shuttle mechanism.

Three compounds, DINOSEB, DINOTERB, and PCP, showed a linear dependence of k_{obs} on C_{tot} over the entire pH range investigated, indicating that the heterodimer was insignificant. For these compounds K^m_{AHA} was set to zero. Four compounds, 34DNP, 245TCP, 345TCP, and 2345TeCP, had a contribution from the monomer and heterodimer in the second-order polynomial model. These data sets were fitted with the complete model by assuming a heterodimer formation constant K^m_{AHA} of 1 kg·mol^{-1}, which is greater than the heterodimer formation constant of PCP estimated by Barstad et al. (*15*), and which is low enough that the assumptions for eqs 12 to 14 are justified ($\alpha^m_{AHA} < 1\%$). Alternatively, one could have modeled the term $K^m_{AHA} \cdot k_{AHA}$ together, which yields the same result.

The translocation rate constants k_{HA}, k_A, and k_{AHA} were determined from the experimental data by a nonlinear fit of eq 47 with the statistics function "Nonlinear Regress" in Mathematica (*29*). They are summarized in Table 1. The initial total surface concentrations Γ° (eq 36) were calculated from the total concentration of uncoupler and the pH, with the membrane-water distribution ratios $K_{mw,HA}$ and $K_{mw,A}$, and acidity constants K^w_a given in Table 1. The fractions of the different species in the membrane were calculated from pH and the acidity constants with eqs 12−14.

A typical plot illustrating the quality of fit is shown in Figure 3, in which the membrane potential decay rate constants, λ_1, which were calculated from the model, are plotted against the experimentally determined k_{obs} for 34DNP. Despite scatter in the data, there is no systematic deviation from the line of unit slope.

Figure 4 illustrates the ability of the model to capture variations in k_{obs} as a function of pH at a given value of C_{tot}. Each of the experimental values in Figure 4 represents one data series at a given pH as shown in Figure 2. The pH-dependent curves pass through a maximum. For compounds whose overall activity is dominated by the heterodimer, as

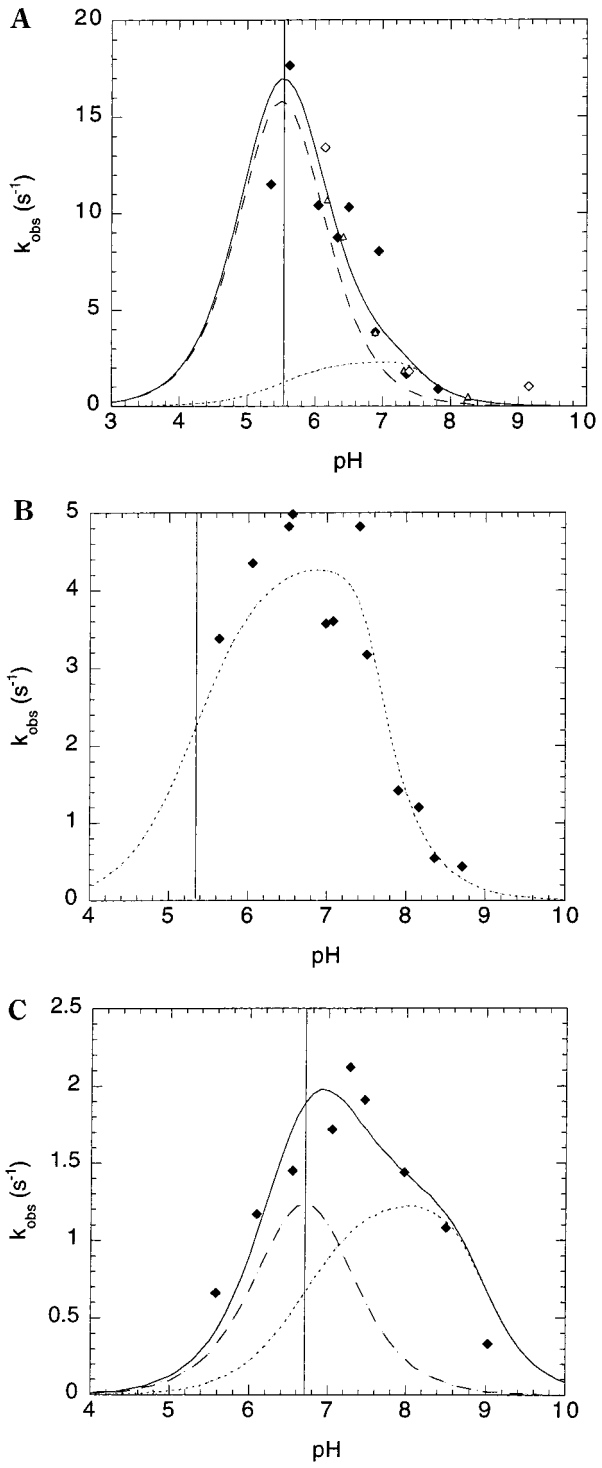

FIGURE 4. Plot of k_{obs} versus pH for (A) 34DNP at $C_{tot} = 5 \cdot 10^{-5}$ M, (B) PCP at $C_{tot} = 10^{-5}$ M, and (C) 2345TeCP at $C_{tot} = 4 \cdot 10^{-6}$ M. The solid line corresponds to the model described by eq 47 and the parameters from Table 1. The broken line and the dotted line represent the contribution of the heterodimer and the phenoxide species, respectively, to the overall activity. The symbols correspond to the experimental values at the given C_{tot}; each point is intrapolated from the simplified quadratic model described by eq 30. The different symbols for the experimental data of 34DNP correspond to experiments with different batches of chromatophores.

is the case for 34DNP (Figure 4A), the maximum of activity is at a pH that corresponds to the pK^m_a in the membrane. Compounds that show only little or no heterodimer formation, e.g. PCP (Figure 4B), has a maximum of activity that is

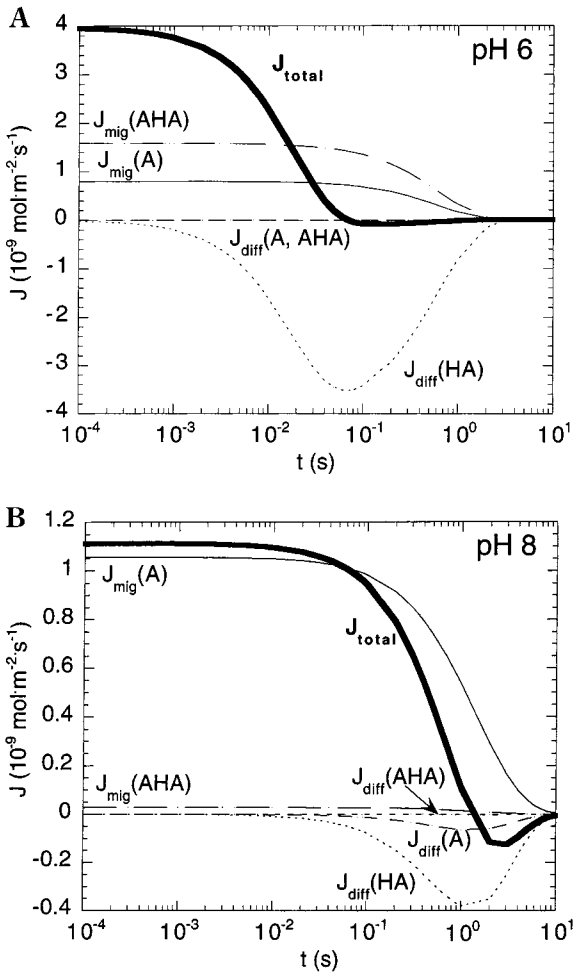

FIGURE 5. Migrational and diffusive fluxes as a function of time for 34DNP at (A) pH 6 and (B) pH 8 calculated for a total concentration of uncoupler $C_{tot} = 15\ \mu M$ and a membrane lipid-to-water ratio [m] of $8.1 \cdot 10^{-4}$ kg·L^{-1}.

shifted to the alkaline side of the pK_a^m. The maximum is broadened by high k_{HA} values. If phenoxide and heterodimer are equally important, the pH range below pK_a^m is dominated by the flux of the heterodimer, and the pH range above pK_a^m is dominated by the flux of the phenoxide ion, and the maximum of activity is between these two maxima as in the case of 2345TeCP (Figure 4C).

The fluxes of all phenolic species can be calculated with eqs 23 and 26−28 with the parameters listed in Table 1 and the appropriate values of pH, C_{tot}, and [m]. These fluxes are depicted in Figure 5 for 34DNP at pH 6 and 8. Positive values of flux correspond to a translocation from surface ′ to surface ″, and negative fluxes to the opposite way. Note that the time scale is logarithmic and that the overall process has a neutral mass balance. Initially, the charged species migrate across the membrane, driven by the membrane potential. At pH 6, the heterodimer is the dominant charged species, and, at pH 8, the monomer dominates the overall migration. At the beginning of the experiment, when the membrane potential is the only driving force and no phenolic species have moved across the membrane, the maximum of loss rate of phenol migrating from one surface to the other is small enough that the concentrations of phenolic species at one surface do not get depleted before back-diffusion starts to occur. The back-diffusion of the neutral phenol and, to a very small extent, phenoxide and heterodimer sets in after 1−10 ms. The potential gradient is destroyed, and the concentrations are reequilibrated within 1−10 s. From Figure 5 it is evident that

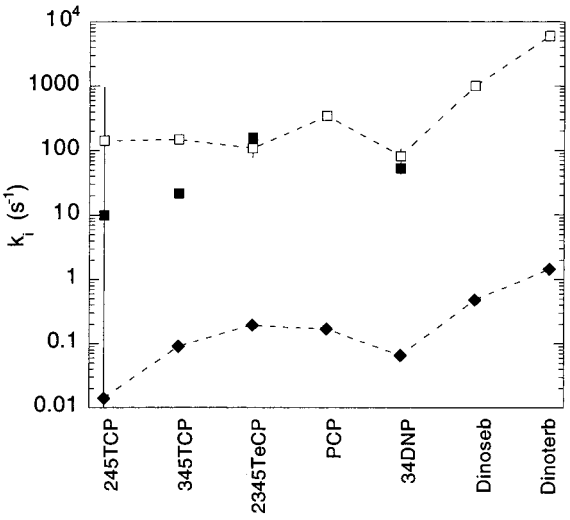

FIGURE 6. The relationship between the translocation rate constants k_{HA} (□), k_A (◆), and k_{AHA} (■) for the compounds investigated.

the simple quadratic model of uncoupling that is based on the flux of the anions as rate-limiting step of the overall process cannot fully explain the protonophoric shuttle mechanism, because the back-diffusion of phenol contributes significantly to the overall process. Note also that at the higher pH values, typically above pH 8, there is a significant theoretical contribution of λ_2 to the overall process which is taken into account in Figure 5B, although it was not possible to resolve the fast decay phase experimentally.

Despite structure-dependent variability of the k_i values of the different compounds investigated, which is discussed in more detail below, there are two distinct ranges of translocation rate constants as shown in Figure 6. The values of k_{HA} are more than 3 orders of magnitude greater than the corresponding k_A, but only about 1 order of magnitude higher than k_{AHA}. Since K_{AHA}^m was set to 1, in fact the product of K_{AHA}^m and k_{AHA} was modeled. The values themselves vary within 1 order of magnitude between the compounds. If a heterodimer is formed at all, the values of k_{AHA} are almost 3 orders of magnitude greater than the values of k_A, which is consistent with the expectation that the dimer has a larger translocation rate constant than the anion because the solubility of an ion increases strongly with size in a medium of low dielectric constant, i.e., in the interior of the lipid membrane. It is difficult to discuss quantitatively this ratio, because the heterodimer formation constant K_{AHA}^m is not known. Although the value of K_{AHA}^m was set to 1 for simplicity of the modeling, one would expect that it is not the same for the different substituted phenols, but it is influenced by geometric parameters. It is more likely that k_{AHA}/k_A is constant because it should depend only on the effective size of the ions. Independent measurements of heterodimer formation constants are required for a more detailed interpretation of this issue. The ratio of k_{HA} to k_A varies much more than the ratio of k_{AHA} to k_A. This result indicates that different factors influence the translocation rates of the neutral and charged species of the same compound. Note that the set of compounds is far too small to allow any definitive conclusions to be reached.

As shown in Figure 6, it is evident that the type and position of the substituents strongly influence the translocation rate constants. The effect of a given substituent on the translocation rate constants is different from its effect on the membrane-water distribution ratio. The most hydrophobic compounds have not necessarily the highest k_A and k_{AHA}. For instance, DINOSEB and DINOTERB have smaller $K_{mw,HA}$ and $K_{mw,A}$ than all chlorophenols but exhibit the highest k_A and

k_{HA}. The charge of DINOSEB and DINOTERB appears to be most effectively distributed over the entire molecule, and the *sec*- and the *tert*-butyl groups shield the hydroxy function sterically. 34DNP has a very low k_A and a significant k_{AHA}, which points to a good delocalization of the charge and a good ability to form heterodimers, but both A and AHA are only slightly membrane permeable because they are rather hydrophilic.

The formation of heterodimers is highly unfavorable for DINOSEB, DINOTERB, and PCP due to the two bulky ortho substituents. Only compounds with either no or just one ortho substituent (i.e., 34DNP, 245TCP, 345TCP, and 2345TeCP) appear to to form heterodimers. The heterodimer increases the overall activity of these compounds, but they still are not as strong uncouplers as the diortho substituted phenols investigated here despite their generally higher hydrophobicity. Phenols without ortho substituents appear to have significantly lower k_A and k_{AHA}, even if the charge can be very well delocalized over the entire molecule as is the case for 34DNP. It can be hypothesized that steric shielding of the charge plays a more important role than charge delocalization for the translocation rates of hydrophobic ions. This view is consistent with the extraordinarily high translocation rates of tetraphenylborate analogues (*13*).

Critical Evaluation of the Uncoupling Model. When one considers that the kinetic uncoupling model was initially developed from charge pulse and voltage-clamp measurements on black lipid bilayer membranes (*11*), it is quite impressive that the model can be applied and extended to a subcellular biological system. However, as expected, the model is less well defined for the biological system than for the planar lipid membrane. A single set of k_{obs} data measured as a function of pH and C_{tot} has to be fit by the complete uncoupling model with two to four adjustable parameters. It is straightforward to derive from this observation that the experimental data need to cover both flanks of the peak-shaped pH-dependent curve to yield good results. Since the experimental pH range is limited to pH 5.2−9.0 due to denaturation of proteins at low pH and fusion of chromatophores at high pH, good fitting results, in particular good estimates of both k_A and k_{AHA} can be obtained only with compounds with a pK_a^w between approximately 5.5 and 7.5, such as 2345TeCP (Figure 4C); exceptions are cases in which there is a structural preference for either species, as is the case for the good heterodimer former 34DNP (Figure 4A) and the preferentially monomeric PCP (Figure 4B). For the purely monomeric uncouplers, compounds with pK_a^w values as low as 4 still yield good modeling results.

The experimental data of the more acidic 2,4-dinitrophenol (pK_a^w of 3.94) (data not shown) could not be fit to the model for three reasons. First, the experimental values cover only the far right flank of the pH-dependent activity curve. Second, both monomeric and dimeric shuttle mechanism contribute to the overall effect. Third, the overall activity in the experimentally available pH range is influenced by baseline toxicity as described below. The k_A of the less acidic compounds, 245TCP and 345TCP, exhibited large errors because no data at pH-values higher than pH 9 could be measured and because both presumably form heterodimers easily.

The model was not very sensitive to changes in values of k_{HA}, although the fitted values of k_{HA} were significantly different for the different compounds and the values did have to be greater than zero and not too high (otherwise the model would have been reduced to the earlier quadratic model of eq 30).

Finally, a good fit of the adjustable parameters can be obtained only for rather strong uncouplers, whose activity is not disturbed by the narcotic effect that constitutes the baseline toxicity of any hydrophobic compound. The activity of two weaker uncouplers, 4-nitrophenol and 3,4-dichlorophenol (data not shown) as well as the activity of 2,4-dinitrophenol could not be modeled satisfactorily because the effective concentrations in the membrane were in the range of critical membrane burdens of the narcotic chemicals (*2*) or slightly below. Even the activities of stronger uncouplers were often underestimated by the model in the outer pH region, indicating a significant contribution of the underlying baseline toxicity. One focus of research presently conducted in our group is to incorporate the contribution of baseline toxicity into the kinetic uncoupling model.

Comparison of Translocation Rate Constants with Membrane Permeabilities from the Literature. The overall membrane permeability of species i, P_i, is defined by Fick's Law

$$J_i = P_i(C_i^{w''} - C_i^{w'}) \tag{31}$$

that is, the rate constant for transport of a species from the aqueous phase on one side of the membrane, through the membrane, to the aqueous phase on the other side. Since it can be assumed that transport through the membrane itself is the rate-limiting step (*12*), the translocation rate constants k_i can be transformed into membrane permeabilities P_i

$$P_i = \frac{K_{mw,i}k_i}{s} \tag{32}$$

where s, the specific surface area of the membrane, is 4.4×10^5 m^2 kg^{-1}. This transformation allows comparison of k_i values with P_i values in the literature.

In Table 2 membrane permeabilities calculated from the k_i values given in Table 1 are compared to literature data from various sources and from different types of measurements. In most cases, the membrane permeabilities for the neutral acids are 3−4 orders of magnitude greater than the permeabilities of the corresponding charged bases.

The calculated membrane permeabilities P_{HA} of the neutral species of substituted phenols are only slightly smaller than the ones deduced for carbonylcyanide *p*-trifluoromethoxyphenylhydrazone (FCCP) by Benz et al. (*11*) from charge-pulse experiments. They are also in the same order of magnitude as the permeabilities of the entire membrane to FCCP and other weak acidic uncouplers that were determined with an alternative method based on pH-dependent membrane potential measurements on planar bilayer membranes (*30*−*33*). The differences between the values from various studies appear to be caused by the structure of the molecules and not by the type of the membrane, because the permeability of neutral species is assumed to be independent of the dielectric constant of the membrane (*11*).

The membrane permeabilities of the neutral species obtained in this study agree not only with the data from biophysical studies on planar lipid bilayers but also with data from biological experiments. The reported diffusion coefficient of ubiquinone between two specific quinone binding sites located on opposite sides on the reaction center complex and the cytochrome bc_1 complex in chromatophores (*34*) is in the same order of magnitude as the diffusion coefficient of DINOSEB and DINOTERB.

In contrast to the membrane permeability of neutral molecules, the permeability of an anion is strongly dependent on the dielectric constant ϵ. It is not clear whether there is an interfacial barrier to A and AHA, so calculations of P_A have to be treated with caution. Nevertheless, our average values of k_A agree well with direct measurements of the membrane permeability of hydrophobic anions in decane-containing planar lipid bilayers from different phospholipids membranes

TABLE 2. Membrane Permeabilities P_{HA} of Substituted Phenols and Other Weakly Acidic Uncouplers

compound	P_{HA} (cm·s^{-1}) between sorption sites[d]	P_{HA} (cm·s^{-1}) entire membrane[i]	P_A (cm·s^{-1}) between sorption sites[d]	P_A (cm·s^{-1}) entire membrane[i]
34DNP	$3\cdot10^{-2}$ [e]		10^{-5} [e]	
DINOSEB	2[e]		$2\cdot10^{-4}$ [e]	
DINOTERB	17[e]		10^{-3} [e]	
245TCP	1[e]		$3\cdot10^{-5}$ [e]	
345TCP	2[e]		$5\cdot10^{-4}$ [e]	
2345TeCP	2[e]		$2\cdot10^{-3}$ [e]	
PCP	10[e]		$1\cdot10^{-3}$ [e]	
FCCP[a]	30−60[f]	50[f]	2[f,m]	
CCCP[b]	17[g]	11[g,j]	0.2[g,m]	$2\cdot10^{-3}$ [j]
DTFB[c]	4[h]			
picric acid		0.4[k]		$7\cdot10^{-6}$ [k]
salicylic acid		0.7[l]		$<10^{-7}$ [l]

[a] Carbonycyanide *p*-trifluoromethoxyphenylhydrazone. [b] Carbonycyanide *m*-chlorophenylhydrazone. [c] 5,6-Dichloro-2-trifluoromethylbenzimidazole. [d] From kinetic measurements of uncoupling. [e] This work; in biological membranes; calculated from data in Table 1 with eq 32. [f] Values from Benz and McLaughlin (*11*). [g] Values from Kasianowicz et al. (*12*). [h] Values from Cohen et al. (*31*). [i] From membrane potential measurements using the method described by LeBlanc(*30*). [j] Phosphatidylcholine/phosphatidylethanolamine/cardiolipin/decane bilayers (*30*). [k] Lecithin/cholesterol/decane bilayers (*32*). [l] Lecithin/decane bilayers (*33*). [m] Chlorodecane-containing planar phosphatidycholine membrane.

(*30*, *32*) (Table 2). The permeability of the FCCP anion, P_A, is 2 orders of magnitude greater in a chlorodecane containing planar lipid membrane ($\epsilon = 4.5$) compared to a decane containing membrane ($\epsilon = 2.1$) (*6*, *35*). The dielectric constant of chromatophore membranes is about 3.8 (*36*). Consequently, permeabilities similar to chlorodecane-containing membranes should be expected for P_A in our system. In contrast to expectation, P_A of the phenoxides are much smaller than P_A of FCCP in chlorodecane-membranes.

Benz (*13*) showed for tetraphenylborate and analogues that the structure of lipophilic ions has a strong influence on their translocation rate constants but only a small influence on their membrane-water distribution ratio. We also find increasing translocation rate constants with increasing size of the ion. The effect is not as large as expected from the example of the tetraphenylborate analogues; tetraphenylborate ions are much larger and spherical, and their charge is presumably much better shielded from the surroundings than it is the case for the phenoxides.

Practical Implications. The results presented here show clearly the relevance of mechanistically based toxicity studies. The combination of uncoupling experiments and membrane-water partitioning experiments together with modeling of the uncoupling mechanism allows one to separate the overall uncoupling effect into various factors that can be related to specific properties of the compound investigated. These factors are on one hand related to the concentration and speciation of the substituted phenols at the target site, the membrane, and, on the other hand, to the intrinsic uncoupling parameters, i.e., translocation constants of all species across the membrane and heterodimer formation constant.

These parameters are the basis for the development of meaningful QSAR equations for uncouplers. Saarikoski et al. (*37*, *38*) developed an empirical model to predict the pH-dependence of the toxicity of substituted phenols toward fish and derived QSARs with the octanol−water partitioning constant K_{ow}, the pH, and the acidity constant pK_a as descriptors. QSARs of the in vitro uncoupling activity of substituted phenols are usually based on one hydrophobicity descriptor (e.g., log K_{ow}), one descriptor for the speciation e.g., pK_a), and one descriptor for the steric effect of ortho substituents (*21*, *39*). The results of the present study rationalize the choice of these descriptors since the intrinsic toxicity is strongly dependent on the presence of shielding ortho substituents for higher translocation rate constants or the absence of ortho substituents for good heterodimer formation. *o*-alkylnitrophenols exhibited the highest intrinsic toxicity of all phenols investigated presumably due to steric shielding of the hydroxy group by the bulky alkyl substituents. Phenols without ortho substituents have smaller translocation rates among phenol and phenoxide species, but their overall intrinsic toxicity is high due to their ability to form heterodimers, whose translocation rate constants are almost 3 orders of magnitude greater than those of the phenoxides. Although the small data set of seven compounds presented here does not allow to deduce any quantitative equations, the generalization deduced above are an important basis for future developments of QSARs.

The quantitative differentiation of uptake and speciation from the intrinsic toxicity is in addition a prerequisite for the development of toxicokinetic models. Toxicokinetic models are a valuable tool for the prediction of the pH-dependent activity of HIOCs (*40*). In a more general sense, toxicokinetic models have been applied in aquatic toxicology to link in vitro responses to effects on whole organisms (*41*). They may find in the future an application in the risk assessment of HIOCs including the extrapolation from one organism to another.

The mechanistic approach presented here should be well suited to investigate the joint effect of mixtures of uncouplers and mixtures of baseline toxicants and uncouplers and to test the hypothesis that synergistic effects could occur if heterodimers are formed by the phenoxide species of a strong acid and the neutral species from another compound.

Finally, the approach presented here allows one to deduce clear classification criteria for the uncoupling potency of any weak organic acids. These criteria include not only hydrophobicity and acidity of a given compound but also additional electronic and steric factors. Further investigations are presently being undertaken in our laboratory to extend the range of tested compounds and to realize the envisaged applications.

Acknowledgments

We are indebted to Mario Snozzi for help with the development of the measuring method and to Philippe Périsset for help with the build-up of the instrument. We thank Jim Anderson, Rik Eggen, Kai Goss, and Nina Schweigert for reviewing the manuscript. Valuable comments were made by Urs Fringeli. This project was supported by a grant of the Swiss Federal Institute of Technology (TH project 0-20-268-96).

Appendix: Mathematical Derivation of the Uncoupling Model

The following derivation of the uncoupling model is in principle applicable to organic acids and bases and may account for heterodimer formation and formation of other complexes. For the organic acids described in this paper, species i refers to HA, A, and AHA.

The total concentration of uncoupler molecules in the membrane, Γ^0 (mol·m^{-2}), during the course of the experiment is assumed to be constant

$$\Gamma^0 = \frac{\sum_i n_i\Gamma_i' + \sum_i n_i\Gamma_i''}{2} \tag{33}$$

where n_i refers to the stoichiometric coefficient (i.e., $n_{HA} = 1$, $n_A = 1$, and $n_{AHA} = 2$). At any time during the experiment, the surface concentration of a single species, Γ_i', is a function of the fraction of this species, α_i^m, in the membrane and the total concentration at the given side of the membrane,

$$\Gamma_i' = \alpha_i^m\Gamma' \tag{34}$$

and the total concentration, Γ', is the sum of the concentrations of all species.

$$\Gamma' = \sum_i n_i\Gamma_i' \tag{35}$$

Before the build-up of the membrane potential, the initial surface concentration, $\Gamma°$, is equal on both sides of the membrane and is the sum of the surface concentration of all species.

$$\Gamma^0 = \sum_i n_i\Gamma_i^{0\prime} = \sum_i n_i\Gamma_i^{0\prime} \tag{36}$$

The function $\Delta\Gamma$, the difference in surface concentrations, is defined by

$$\Delta\Gamma = \frac{\sum_i n_i\Gamma_i'' - \sum_i n_i\Gamma_i'}{2} \tag{37}$$

To make the concentration term $\Delta\Gamma$ dimensionless, the function $\Delta\Theta$ is introduced, which corresponds to the fractional coverage of the surface:

$$\Delta\Theta = \frac{\Delta\Gamma}{\Gamma^0} \tag{38}$$

With a combination of eqs 33 and 38, the flux equation (eq 23) can be rewritten as

$$J_i = -2k_i\alpha_i^m\Gamma^0\Delta\Theta - k_i\alpha_i^m\Gamma^0 z_i\Delta u \tag{39}$$

and the differential equation for $\Delta\Theta$ is derived from eqs 23, 37, and 38 and amounts to

$$\frac{d\Delta\Theta}{dt} = \frac{1}{\Gamma^0}\sum_i n_iJ_i \tag{40}$$

or upon substitution of eq 39 for J_i

$$\frac{d\Delta\Theta}{dt} = -2(\sum_i n_ik_i\alpha_i^m)\Delta\Theta - (\sum_i n_ik_i\alpha_i^m z_i)\Delta u \tag{41}$$

Conversion of the differential equation for the change in surface charge (eq 25) to the dimensionless membrane potential Δu (eqs 22 and 24) yields the following differential equation

$$\frac{d\Delta u}{dt} = \frac{F^2}{CRT}\sum_i z_iJ_i \tag{42}$$

which can be rearranged, upon substitution of eq 39 for J_i, to

$$\frac{d\Delta u}{dt} = -2B(\sum_i k_i\alpha_i^m z_i)\Gamma^0\Delta\Theta - B(\sum_i k_i\alpha_i^m z_i^2)\Gamma^0\Delta u \tag{43}$$

where

$$B = \frac{F^2}{CRT} \tag{44}$$

The solution of the linear nonhomogeneous differential equation system that consists of eqs 41 and 43 is of the following form:

$$\Delta\Theta(t) = b_1e^{\lambda_1 t} + b_1e^{\lambda_2 t} \tag{45}$$

$$\Delta u(t) = b_1u_1e^{\lambda_1 t} + b_2u_2e^{\lambda_1 t} \tag{46}$$

The eigenvalues λ_1 and λ_2 correspond to the two expected rate constants of decay of membrane potential.

$$\lambda_{1,2} = 0.5\left(-2(\sum_i n_ik_i\alpha_i^m) - B(\sum_i k_i\alpha_i^m z_i^2)\Gamma^0 \pm \sqrt{(-2(\sum_i n_ik_i\alpha_i^m) + B(\sum_i k_i\alpha_i^m z_i^2)\Gamma^0)^2 + 8B(\sum_i n_ik_i\alpha_i^m z_i)(\sum_i k_i\alpha_i^m z_i)\Gamma^0}\right) \tag{47}$$

The initial conditions are $\Delta u(t{=}0) = u_0$ and $\Delta\Theta(t{=}0) = 0$, i.e., no reaction before the potential build-up induced by the flash. The relaxation amplitudes are then given by

$$u_1 = \frac{\lambda_1 + 2(\sum_i n_ik_i\alpha_i^m)}{\sum_i n_ik_i\alpha_i^m z_i} \tag{48}$$

$$u_2 = \frac{\lambda_2 + 2(\sum_i n_ik_i\alpha_i^m)}{\sum_i n_ik_i\alpha_i^m z_i} \tag{49}$$

$$b_1 = \frac{-\sum_i n_ik_i\alpha_i^m z_i}{\lambda_1 - \lambda_2}u_0 \tag{50}$$

Since the membrane is isolated toward the aqueous phase, it follows that $b_2 = -b_1$.

Literature Cited

(1) Escher, B. I.; Behra, R.; Eggen, R. I. L.; Fent, K. *Chimia* **1997**, *51*, 915−921.

(2) van Wezel, A.; Opperhuizen, A. *Crit. Rev. Toxicol.* **1995**, *25*, 255−279.

(3) Verhaar, H. J. M.; van Leeuwen, C. J.; Hermens, J. L. M. *Chemosphere* **1992**, *25*, 471−491.
(4) Escher, B. I.; Snozzi, M.; Häberli, K.; Schwarzenbach, R. P. *Environ. Toxicol. Chem.* **1997**, *16*, 405−414.
(5) Terada, H. *Environ. Health Perspect.* **1990**, *87*, 213−218.
(6) McLaughlin, S. G. A.; Dilger, J. P. *Physiol. Rev.* **1980**, *60*, 825−863.
(7) Finkelstein, A. *Biochim. Biophys. Acta* **1970**, *205*, 1−6.
(8) Crielaard, W.; van Mourik, F.; van Grondelle, R.; Konings, W. N.; Hellingwerf, K. J. *Biochim. Biophys. Acta* **1992**, *1100*, 9−14.
(9) Escher, B. I.; Snozzi, M.; Schwarzenbach, R. P. *Environ. Sci. Technol.* **1996**, *30*, 3071−3079.
(10) Escher, B. I.; Schwarzenbach, R. P. *Environ. Sci. Technol.* **1996**, *30*, 260−270.
(11) Benz, R.; McLaughlin, S. *Biophys. J.* **1983**, *41*, 381−398.
(12) Kasianowicz, J.; Benz, R.; McLaughlin, S. *J. Membrane Biol.* **1984**, *82*, 179−190.
(13) Benz, R. *Biophys. J.* **1988**, *54*, 25−33.
(14) Kasianowicz, J.; Benz, R.; McLaughlin, S. *J. Membr. Biol.* **1987**, *95*, 73−89.
(15) Barstad, A. W.; Peyton, D. H.; Smejtek, P. *Biochim. Biophys. Acta* **1993**, *1140*, 262−270.
(16) Bäuerle, H.; Seelig, J. *Biochemistry* **1991**, *30*, 7203−7211.
(17) Seelig, J.; Ganz, P. *Biochemistry* **1991**, *30*, 9354−9359.
(18) Birrell, G. B.; Sistrom, W. R.; Griffith, O. H. *Biochemistry* **1978**, *17*, 3768−3773.
(19) Casadio, R.; Venturoli, G.; Melandri, B. A. *Eur. J. Biophys.* **1988**, *16*, 243−253.
(20) Crofts, A. R.; Wraight, C. A. *Biochim. Biophys. Acta* **1983**, *726*, 149−185.
(21) Escher, B. I. Ph.D. thesis, Swiss Federal Institute of Technology, Zürich, Switzerland, 1995.
(22) Junge, W.; Jackson, J. B. In: *Photosynthesis: Energy Conversion by Plants and Bacteria*; Govindjee, Ed.; Academic Press: New York, 1982; Vol. 1, pp 589−646.
(23) Melandri, B. A.; Mehlhorn, R. J.; Packer, L. *Arch. Biochem. Biophys.* **1984**, *235*, 97−105.
(24) Albert, A.; Serjeant, E. P. *The determination of ionization constants*; Chapman and Hall: London, UK, 1984.
(25) Schwarzenbach, R. P.; Stierli, R.; Folsom, B. R.; Zeyer, J. *Environ. Sci. Technol.* **1988**, *22*, 83−92.
(26) Schellenberg, K.; Leuenberger, C.; Schwarzenbach, R. P. *Environ. Sci. Technol.* **1984**, *18*, 652−657.
(27) Miyoshi, H.; Nishioka, T.; Fujita, T. *Biochim. Biophys. Acta* **1987**, *891*, 194−204.
(28) Escher, B. I.; Westall, J. C.; Schwarzenbach, R. P. Manuscript in preparation.
(29) Wolfram, S. *Mathematica*; Wolfram Research: Champaign, IL, 1996.
(30) LeBlanc, O. H. *J. Membr. Biol.* **1971**, *2*, 227−251.
(31) Cohen, F. S.; Eisenberg, M.; McLaughlin, S. *J. Membr. Biol.* **1977**, *37*, 361−396.
(32) McLaughlin, S.; Eisenberg, M.; Cohen, F.; Dilger, J. In *Frontiers of Biological Energetics*; Dutton, P. L., Leigh, J. S., Scarpa, A., Eds.; Academic: New York, 1978; Vol. 2, pp 1205−1214.
(33) Gutknecht, J.; Tosteson, D. C. *Science* **1973**, *182*, 1258−1261.
(34) Crofts, A. R.; Meinhardt, S. W.; Jones, K. R.; Snozzi, M. *Biochim. Biophys. Acta* **1983**, *723*, 202−218.
(35) Dilger, J.; McLaughlin, S.; McIntosh, T.; Simon, S. *Science* **1979**, *206*, 1196−1198.
(36) Packham, N. K.; Berriman, J. A.; Jackson, J. B. *FEBS Lett.* **1978**, *89*, 205−210.
(37) Saarikoski, J.; Viluksela, M. *Arch. Environ. Contam. Toxicol.* **1981**, *10*, 747−753.
(38) Saarikoski, J.; Viluksela, M. *Ecotoxicol. Environ. Saf.* **1982**, *6*, 501−512.
(39) Miyoshi, H.; Fujita, T. *Biochim. Biophys. Acta* **1988**, *935*, 312−321.
(40) Howe, G. W.; Marking, L. L.; Bills, T. D.; Rach, J. J.; Mayer Jr., F. L. *Environ. Toxicol. Chem.* **1994**, *13*, 51−66.
(41) McKim, J. M.; Nichols, J. W. In: *Aquatic Toxicology: Molecular, Biochemical, and Cellular Aspects*; Malins, D. D., Ostrander, G. K., Eds.; Lewis: Boca Raton, FL, 1994; pp 469−519.

Received for review May 27, 1998. Revised manuscript received November 4, 1998. Accepted November 12, 1998.

ES980545H